

The isothermal section of the Er–Fe–Sb ternary system at 773 K

Gemei Cai^{a,b}, Xiangzhong Wei^c, Lingmin Zeng^{a,b,*}

^a Institute of Materials Science, Guangxi University, Nanning Guangxi 530004, PR China

^b Key Laboratory of Nonferrous Metal Materials and New Processing Technology, Ministry of Education, Guangxi University, Nanning, Guangxi 530004, PR China

^c Guangxi Traditional Chinese Medical University, Nanning, Guangxi 530001, PR China

Received 19 July 2005; received in revised form 21 October 2005; accepted 25 October 2005

Available online 27 December 2005

Abstract

The phase relation of the Er–Fe–Sb ternary system at 773 K has been investigated mainly by means of X-ray powder diffraction with the aid of optical microscopy and differential thermal analysis. This section consists of 12 single-phase regions, 22 two-phase regions and 11 three-phase regions. A ternary compound Er₆FeSb₂ has been confirmed.

© 2005 Elsevier B.V. All rights reserved.

Keywords: Er–Fe–Sb; Phase relation; X-ray diffraction

1. Introduction

Our group has investigated the phase relationship and the crystal structure of the RE–T (transition elements)–Sb ternary system systematically [1–5]. The partial phase diagram in the Er–Fe–Sb system (Sb ≤ 50 at.%) at 1173 K and a ternary compound Er₆FeSb₂ were reported [6]. The binary diagrams of the Er–Fe, Er–Sb and Fe–Sb systems bounding the Er–Fe–Sb are presented in [7]. At 773 K, there are four intermediate phases Fe₁₇Er₂, Fe₂₃Er₆, Fe₃Er, Fe₂Er in the Er–Fe binary system, two compounds ErSb and Er₅Sb₃ in the Er–Sb system, and two intermediate phases FeSb, FeSb₂ in the Fe–Sb system. In this paper, we report the isothermal section of the Er–Fe–Sb ternary system at 773 K.

2. Experimental

For sample preparation, the purity of Er, Fe and Sb used in this work is 99.9, 99.9, and 99.95%, respectively. Most of samples, having masses of 3 g, were prepared in an electric arc furnace under high pure argon atmosphere using a non-consumable tungsten electrode and a water-cooled copper crucible. The Sb-rich alloys were melted by induction melting in a sintered Al₂O₃ crucible under high pure argon atmosphere. As Sb is easy to volatilize, before melting an extra amount of Sb was added to compensate for the weight loss. During melting, we used the electric current as low as possible to minimize the loss of antimony by

vaporizing. All alloys after melting were subjected to a homogenizing anneal in evacuated quartz tube. The samples with more than 40 at.% Er were annealed at 1123 K for 240 h, the samples with more than 40 at.% Fe were annealed at 1093 K for 300 h and the samples with more than 60 at.% Sb were annealed at 773 K for 25 days. Then, they were cooled at a rate of 10 K/h to 773 K and kept there for 1 week, finally, quenched into liquid nitrogen.

X-ray powder diffraction and optical microscope were used to analyze the samples. The samples were ground to powder not coarse than 40 μm, and annealed in an evacuated tube for 5 days at 600 K to remove the lattice strains produced by the grinding. The X-ray powder diffraction was performed on a Rigaku D/Max 2500 V diffractometer with Cu Kα radiation and graphite monochromator operated at 40 kV, 250 mA. The Materials Data Inc. software Jade 5.0 [8] and the Powder Diffraction File (PDF release 2002) were used for the phase analysis.

3. Results and discussion

3.1. Binary system

In this work, we have studied the binary systems Er–Fe, Er–Sb and Fe–Sb at 773 K to identify binary compounds before the ternary phase analysis. In the Er–Fe system, four binary compounds Fe₁₇Er₂ [9], Fe₂₃Er₆ [10], Fe₃Er [9], Fe₂Er [9] were confirmed.

In the Er–Sb system, we confirmed the existence of ErSb and Er₅Sb₃ at 773 K. This result is in good agreement with that reported in [7].

In the Fe–Sb binary system, we observed two binary compounds Fe_{1+x}Sb and FeSb₂. It was observed that there was solid

* Corresponding author.

E-mail address: lmzeng@gxu.edu.cn (L. Zeng).

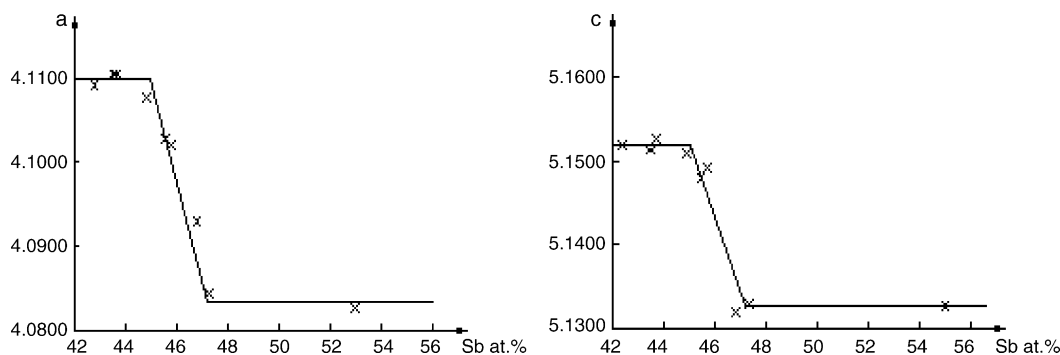


Fig. 1. Determination of the maximum solid solubility of Fe_{1+x}Sb by means of lattice parameters.

Table 1
The variation of lattice parameter of $\text{Fe}_{1-x}\text{Sb}_x$

Samples	Lattice parameters	
	a (Å)	c (Å)
$\text{Fe}_{57.6}\text{Sb}_{42.4}$	4.1097 (3)	5.1520 (3)
$\text{Fe}_{56.45}\text{Sb}_{43.55}$	4.1110 (4)	5.1512 (5)
$\text{Fe}_{56.33}\text{Sb}_{43.67}$	4.1119 (3)	5.1529 (4)
$\text{Fe}_{55.12}\text{Sb}_{44.88}$	4.1082 (6)	5.1511 (9)
$\text{Fe}_{54.39}\text{Sb}_{45.61}$	4.1031 (2)	5.1484 (2)
$\text{Fe}_{54.21}\text{Sb}_{45.79}$	4.1027 (4)	5.1494 (4)
$\text{Fe}_{53.19}\text{Sb}_{46.81}$	4.0926 (4)	5.1319 (4)
$\text{Fe}_{52.64}\text{Sb}_{47.36}$	4.0843 (3)	5.1329 (3)
$\text{Fe}_{45}\text{Sb}_{55}$	4.0825 (3)	5.1323 (4)

Table 2
Details of the phase regions in the Er–Fe–Sb ternary system at 773 K

Samples	Fe (at.%)	Er (at.%)	Sb (at.%)	Phase composition
1	94	6	0	Fe + $\text{Fe}_{17}\text{Er}_2$
2	84	16	0	$\text{Fe}_{17}\text{Er}_2$ + $\text{Fe}_{23}\text{Er}_6$
3	77	23	0	$\text{Fe}_{23}\text{Er}_6$ + Fe_3Er
4	71	29	0	Fe_3Er + Fe_2Er
5	50	50	0	Fe_2Er + Er
6	30	70	0	Er + Fe_2Er
7	0	80	20	Er + Er_5Sb_3
8	0	60	40	Er_5Sb_3 + ErSb
9	0	33.3	66.7	ErSb + Sb
10	20	0	80	Sb + FeSb_2
11	40	0	60	FeSb_2 + FeSb
12	80	0	20	FeSb + Fe
13	60	22	18	Fe + $\text{Fe}_{17}\text{Er}_2$ + ErSb
14	60	26	14	$\text{Fe}_{17}\text{Er}_2$ + $\text{Fe}_{23}\text{Er}_6$ + ErSb
15	52	32	16	$\text{Fe}_{23}\text{Er}_6$ + Fe_3Er + ErSb
16	48	36	16	Fe_3Er + Fe_2Er + ErSb
17	40	46	14	Fe_2Er + Er_6FeSb_2 + Er_5Sb_3
18	10	52	38	Er_5Sb_3 + ErSb + Fe_2Er
19	20	70	10	Fe_2Er + Er_6FeSb_2 + Er
20	6	70	24	Er_6FeSb_2 + Er + Er_5Sb_3
21	10	20	70	Sb + FeSb_2 + ErSb
22	24	20	56	FeSb_2 + FeSb + ErSb
23	40	20	40	FeSb + Fe + ErSb

solubility of Sb in Fe_{1+x}Sb . In order to determine this range, nine powder samples of Fe_{1+x}Sb were prepared. After adding adequate highly pure silicon powder to these samples as an internal standard, we collected the X-ray powder diffraction data. The lattice parameters were refined by using the Jade 5.0 program and listed in Table 1. The variation of the lattice parameters of FeSb with Sb is shown in Fig. 1. From Fig. 1, we concluded that the maximum solid solubility of Sb in Fe_{1+x}Sb was about 2.2%.

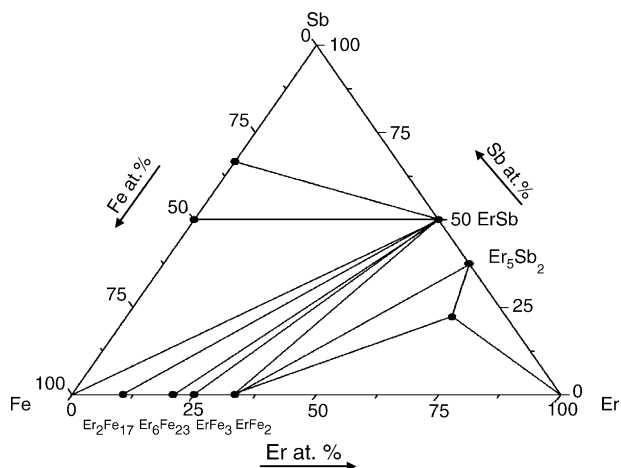


Fig. 2. The isothermal section of the Er–Fe–Sb ternary system at 773 K.

Table 3
Crystallographic data of the initial components and binary compounds for the Er–Fe–Sb at 773 K

Phase	PDF no.	Space group	Lattice parameters			Reference
			a (Å)	b (Å)	c (Å)	
Fe	87–22	$Im\bar{3}m$	2.860	–	–	[11]
$\text{Fe}_{17}\text{Er}_2$	65–080	$P6_3/mmc$	8.430	–	8.279	[9]
$\text{Fe}_{23}\text{Er}_6$	–	$Fm\bar{3}m$	11.994	–	–	[10]
Fe_3Er	43–373	$R\bar{3}m$	5.086	–	24.46	[9]
Fe_2Er	65–758	$Fd\bar{3}m$	7.283	–	–	[9]
Er	65–866	$P6_3/mmc$	3.558	–	5.587	[12]
Er_5Sb_3	–	$Pm\bar{3}m$	11.674	9.156	8.004	This work
ErSb	–	$Fm\bar{3}m$	6.106	–	–	[13]
Sb	85–322	$R\bar{3}m$	4.308	–	11.274	[14]
FeSb_2	80–430	$Pnn2$	5.832	6.537	3.197	[15]
εFeSb	–	$P6_3/mmc$	4.07	–	5.13	[16]
FeEr_6Sb_2	–	$P6_2m$	8.091	–	4.125	This work

3.2. The phase relationship of the Er–Fe–Sb system at 773 K

The isothermal section of the Er–Fe–Sb ternary system at 773 K has been determined (Fig. 2) on the basis of our X-ray data and metallographic results. There are 11 three-phase regions, 22 two-phase regions and 12 single-phase regions in this section. A ternary compound Er_6FeSb_2 has been confirmed. Details of the two-phase and three-phase regions were given in Table 2. The structural information of the phases in the Er–Fe–Sb system at 773 K was listed in Table 3.

Acknowledgement

This work was supported by the National Natural Science Foundation of China (Grant no. 59971018).

References

- [1] L. Zeng, L. Tan, J. Alloys Compd. 346 (2002) 197–199.
- [2] L. Zeng, S. Wang, J. Alloys Compd. 351 (2003) 176–179.
- [3] L. Zeng, H. Ning, J. Alloys Compd. 359 (2003) 169–171.
- [4] L. Zeng, H. Zhao, J. Alloys Compd. 366 (2004) 201–204.
- [5] L. Zeng, X. Xie, J. Alloys Compd. 365 (2004) 178–180.
- [6] A.V. Morozkin, J. Alloys Compd. 373 (2004) 3–4.
- [7] T.B. Massalski, Binary Alloy Phase Diagrams, ASM International, Materials Park, OH, 1990.
- [8] Jade 5.0, XRD Pattern Processing Materials Data Inc., 1999.
- [9] K.H.J. Buschow, A.S. Van Der Goot, Phys. Status Solidi. 35 (1969) 515–522.
- [10] J.F. Herbst, J.J. Croat, B. van Laar, W.B. Yelon, J. Appl. Phys. 56 (1984) 1224–1226.
- [11] E.A. Owen, G.I. Williams, J. Sci. Instrum. 31 (1954) 49.
- [12] F.H. Spedding, A.H. Daane, K.W. Herrmann, Acta Crystallogr. 9 (1956) 559.
- [13] F. Lévy, Physik Der Kondensierten Materie 10 (1969) 85–106.
- [14] C.S. Barrett, P. Cucka, K. Haefner, Acta Crystallogr. 16 (1963) 451–453.
- [15] H. Holseth, A. Kjekshus, Acta Chem. Scand. 23 (1969) 3043–3050.
- [16] R. Kumar, K.S. Harchand, K. Vishwamittar, P. Chandra, T. Jernberg, R. Ericsson, Wäppling, Phys. Rev. B: Condensed Matter 32 (1985) 69–75.